Investigation of Supersonic Turbulent Mixing Layer with Zero Pressure Gradient

HIDEO IKAWA* AND TOSHI KUBOTA†
California Institute of Technology, Pasadena, Calif.

The effect of compressibility on the mixing layer was investigated at Mach number 2.47. Pitot pressure, static pressure, and hot-wire surveys were conducted to investigate the mean flow and the fluctuation quantities. Similarities between supersonic and incompressible mixing layers were observed in normalized velocity profile, normalized power spectral density distribution, and convection velocity distribution. Spreading rate, normalized shear stress, and velocity fluctuation were found to be appreciably smaller than the respective incompressible results; e.g., the momentum thickness growth rates are 0.0073 and 0.035 for supersonic and incompressible flows, respectively. The difference between free and wall-bounded mixing layers is discussed. Development of turbulence structure of mixing layer with increasing Reynolds number was also investigated.

Nomenclature

A = area of porous plate, in.^{2}
b = width of mixing layer, in.
e = voltage fluctuation, mv
E_{tc} = hot-wire thermocouple output, mv
f = frequency, Hz
M = Mach number
M_A = compensating amplifier time constant, μsec
M_t = hot-wire thermal lag time constant, μsec
$\dot{m}_{ACT}$ = injected mass flux through porous plate
p = pressure, mmHg
p_o = stagnation pressure, mmHg
$R_{u'T'}$ = correlation coefficient of velocity and temperature fluctuation
$S_\pi, S_u^*, S_\rho, S_{T_o}$ = hot-wire sensitivity coefficients of pressure, velocity, density, and temperature fluctuations
T = temperature, °F or °K
U = freestream velocity, fps
u, v, w = velocity components
x, y, z = axial, lateral, spanwise coordinate
$\bar{x}, \bar{y}, \bar{z}$ = incompressible coordinate
X_E = axial distance measured from the virtual origin
X_{E_R} = reference axial distance measured from the virtual origin (= 7.25 in.)
θ = momentum thickness $= \int_{-\infty}^{\infty} (\rho u/\rho_e u_e)(1-u/u_e)\,dy$
θ_o = initial momentum thickness of boundary layer at step corner, in.
Λ = integral scale
λ_e = mass entrainment rate $= \dot{m}_{ACT}/A\rho_e u_e$
σ = spreading parameter $(\sigma y/x)$
ρ = density of fluid, slug/ft^3
τ = shear stress
π' = static pressure fluctuation $p'/\gamma p$
γ = ratio of specific heats

Superscripts

$(\ )'$ = fluctuation quantity
$(\ )'^2$ = mean-squared fluctuation quantity $\overline{g'^2}$
$(\tilde{\ })'^2$ = normalized mean-squared quantity $\tilde{g}'^2 = \overline{g'^2} \Big/ \int_o^\infty \overline{g'^2}\,df$
$(\ )^*$ = dividing streamline
$\langle\ \rangle$ = rms fluctuation quantity $(\overline{g'^2})^{1/2}$

Subscripts

c = convection flow quantity
e = edge condition of TFML
L = local flow property
o = stagnation flow quantity
w = lower boundary condition of TFML

Definitions

F-T-F = boundary-layer trip with fine grain sandpaper (carborandum C-320)
R-T-F = boundary-layer trip with coarse grain sandpaper (alum-oxide EC #30)
TBL = turbulent boundary layer
TFML = turbulent free mixing layer
TWML = turbulent wall (forced) mixing layer
H-D transformation = Howarth-Dorodnitsyn transformation $\left(\bar{y} = \int_o^y (\rho/\rho_e)\,dy\right)$

Presented as Paper 74-40 at the AIAA 12th Aerospace Sciences Meeting, Washington D.C., January 30–February 1, 1974; submitted February 28, 1974; revision received August 29, 1974. This research was sponsored by the U.S. Army Research Office and the Advanced Research Projects Agency, Contract DA-31-124-ARO(D)-33 and DAHC 04-72-C-0038.

Index categories: Supersonic and Hypersonic Flow; Jets, Wakes and Viscid-Inviscid Flow Interactions.

* Graduate Student, Aeronautics. Member AIAA.
† Professor of Aeronautics. Member AIAA.

Introduction

In the past two and a half decades, extensive investigations have been conducted to broaden the knowledge of the two-dimensional supersonic turbulent mixing layer. Many experiments, summarized by Maydew and Reed,[1] were conducted in the mixing region of a jet. Two-dimensional mixing layers in wind tunnels were investigated by Roshko and Thomke[2] and by Sirieix and Solignac.[3] However, these investigations were limited to measurements of the mean velocity profiles and the growth rates of the turbulent mixing layer. The problem was theoretically investigated[4–6] to determine the compressibility effect on the velocity profile and spreading rate of the turbulent mixing layer. The general conclusions drawn from these investigations are: 1) the spreading rate (and hence the mass entrainment rate) decreases with increasing Mach number, and 2) the velocity profile can be reduced to the incompressible form by scaling the lateral coordinate by the Mach number dependent spreading parameter, σ. Contrary to these findings, the mixing-layer type flow created by a uniform injection of air into the supersonic turbulent boundary layer investigated by Fernandez[7] revealed that: 1) the mass entrainment rate was Mach number independent, and 2) supersonic velocity profiles can be reduced to the incompressible

form by applying the Howarth-Dorodnitsyn transformation to the lateral coordinate. The present investigation[8] was undertaken in order to clarify the dependence of the turbulent mixing layer properties on Mach number and to obtain a measurement of the streamwise component of the fluctuation field.

Description of Experiments

The experiments were conducted in the supersonic ($M_e = 2.47$) wind tunnel of the Graduate Aeronautical Laboratories, California Institute of Technology (GALCIT). Pertinent operational conditions are shown in Fig. 1. The velocity and pressure fluctuations, measured in the undisturbed flow upstream of the step, were found to be 0.2% of the freestream velocity and 0.1% of the dynamic pressure, respectively.

An ideal, constant pressure supersonic mixing layer with minimum flow interference was created downstream of the rearward facing step in the setup shown in Fig. 1. This was accomplished by injecting a controlled amount of air uniformly into the base region through the porous plate until the pressure levels between the upstream and the base regions were equalized. An undesirable pressure gradient induced by the abrupt termination of an injection at the end of the plate was eliminated by installing a precisely contoured block simulating the streamline which exists downstream of the injection plate. The mass entrainment rate through the lower boundary of the mixing layer was also precisely measured with the present arrangement. Uniformity of the flow through the porous plate was investigated by means of a hot-wire probe. A small-scale spatial variation of less than 5% of the mean flow was detected near the surface but was damped out quickly with increasing height above the surface.

Distribution of the mean flow properties in the mixing layer was measured by the Pitot and static pressure surveys. In order to monitor the probe interference on the flow during the test, one of the side fences was instrumented with 40 static pressure taps. The total temperature distribution was measured with the hot-wire operating as a resistance thermometer. The wire Nusselt number needed to compute the Mach number-dependent sensitivity coefficients of the hot-wire measurement were also measured across the mixing layer.

The turbulent fluctuations of the streamwise component were measured by the Shapiro-Edward constant current hot-wire anemometer. The hot-wire probes were made of 0.00005 in. diam platinum-10% rhodium wire with a ratio of length to diameter ranging from 120 to 200. The unresolved turbulent quantities were measured directly with the thermocouple power meter (E_{tc}) built in the Shapiro-Edward set and also obtained indirectly by integrating the power spectral density distribution measured with the Tektronix Spectrum Analyzer Type 1L5. A set of turbulence measurements with a minimum of six overheats was obtained at each sampling point.

The crosscorrelations of two hot-wire signals, arranged in tandem along a ray of the constant velocity, were made to determine the convection velocity profile. The measurements were taken with the SAICOR Correlation and Probability Analyzer (Model SAI 43A) during the experiment.

Data Reduction

Mean flow quantities were computed by the Pitot-Rayleigh formula with constant total temperature and constant static pressure assumptions across the mixing layer. A small deviation of the static pressure (less than 2% of mean) did not appreciably alter the velocity profile or the spreading rate. The dividing streamline was determined from the profile measurement by balancing the momentum of upper and lower regions across the free shear layer with respect to the dividing streamline.

$$\int_{-\infty}^{y^*} \frac{\rho u}{\rho_e u_e} dy = \int_{-\infty}^{\infty} \frac{\rho u}{\rho_e u_e}\left(1 - \frac{u}{u_e}\right) dy - \theta_o \qquad (1)$$

The dividing streamline was also determined by the mass balance.

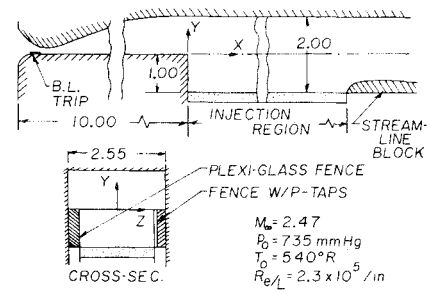

Fig. 1 Test section.

$$\int_{-\infty}^{y^*} (\rho u/\rho_e u_e)\, dy = \int_o^x \lambda_e\, dx \qquad (2)$$

The mass entrainment rate (λ_e) was determined from the measured injection rate. Since λ_e and the momentum thickness (θ) were known from the experiment, the location of the dividing streamline, y^*, was determined by the requirement that the mass flux term satisfies Eqs. (1) and (2).

A modal separation of the turbulence quantities was accomplished by Morkovin's curve-fitting technique described by Gran.[9] In the mixing layer, where the local Mach number is less than two ($M_L \leqq 2.0$), the sensitivity coefficients of velocity and density fluctuations become independent of each other, ($e' = -S_u u' - S_\rho \rho' + S_{T_o} T_o'$), and the mean-square voltage fluctuation becomes a linear combination of six unknown products of fluctuating quantities with squares and products of S's as coefficients. In principle, the solutions can be obtained by an inversion of six simultaneous equations constructed by the measurement taken with six overheats, since the hot-wire sensitivity coefficients change with the overheat. However, the near-proportionality of S_u and S_ρ (i.e., $S_\rho \cong KS_u$) prevented the solution by a direct matrix inversion. In practice, this matrix property conveniently enabled us to use the curve-fitting technique for the entire Mach number regime.[8] The mean-square voltage of the unresolved turbulence field, measured by the built-in thermocouple (E_{tc}), was not corrected for amplifier attenuation at high frequencies (amplifier response is flat up to 100 kHz and down to half power at 300 kHz). The correction for the thermal lag of the wire was only approximate in the E_{tc} measurement, unless the time constant of the compensating amplifier (M_A) was set precisely equal to the wire time constant in the local flow (M_t). The modal separation was carried out at several frequencies including compensations for these effects and the spectra of each turbulence component was integrated to obtain the respective intensities.

Within the mixing layer, the velocity and the static temperature fluctuation intensities were calculated by the modified Kistler's method[10] with the assumption that pressure fluctuations (p') are negligible compared with vorticity and entropy fluctuations [i.e., $(S_\pi/S_{T_o})^2\overline{\pi'^2} \leqq 0.04(S_u^*/S_{T_o})^2\overline{u'^2}$]. The effect of p' increases the magnitude of rms velocity fluctuation if u' and p' are highly anticorrelated. Otherwise, the contribution of p' is to reduce the magnitude of rms u'. For example, if $p'/\gamma p$ is assumed to be constant across the TFML and is equalled to the value measured in the freestream, rms u' obtained near the dividing streamline is approximately 10% higher than the value obtained by neglecting the p' term, provided $R_{u'p'} = -1.0$. The convection velocity was determined by the method employed by Wills.[11]

Results and Discussion

Preliminary Mean Flow Measurements

Preliminary investigations of the supersonic turbulent free mixing layer (TFML) were conducted behind a rearward facing step with positioning of the porous wall at two heights. The step height was found to influence the flowfield through the difference in the interaction between the lower edge of the mixing layer and the bottom wall. With a 1-in. step height, the mixing layer

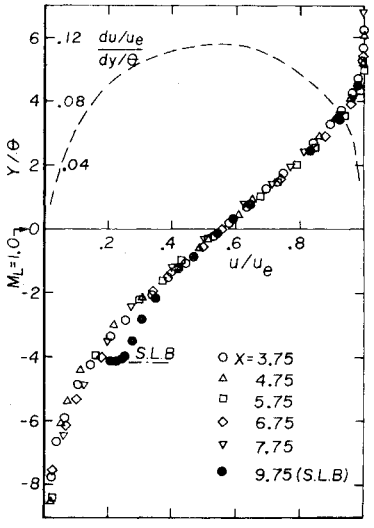

Fig. 2 TFML velocity and velocity gradient profiles.

touched the bottom wall downstream of the porous plate and created a negative pressure gradient on the aft-half of the plate. On the other hand, with a $\frac{1}{2}$-in. step height, the interaction occurred on the porous plate inducing a positive pressure gradient downstream. This observation led to the design of the tailored streamline block as shown in Fig. 1.[8] Preliminary tests revealed the following important findings: In the region where a nearly constant pressure exists, the TFML was remarkably self similar (i.e., a linear growth) and the entrainment rate was considerably lower than the incompressible TFML of Liepmann and Laufer.[12]

Mean Flow Data

Self-similar two-dimensional turbulent mixing layers with zero pressure gradient must satisfy two criteria; the mixing layer spreads linearly with the streamwise distance (x) and the mass entrainment rate through the lower boundary of the mixing layer equals the momentum thickness growth rate ($\lambda_e = d\theta/dx$).

The self-similar flow was established at approximately 275 θ_o downstream of the step in the present investigation. The normalized velocity profiles over the range of $375\theta_o$ to $975\theta_o$ are shown in Fig. 2. The dividing streamline was located near the sonic point. The velocity profile taken at $x = 975\theta_o$, measured over the streamline block, matched with the other profiles demonstrating the effectiveness of flow simulation by artificial means. Another property of the self-similarity is observed in the velocity field map as shown in Fig. 3. The linear growth of the mixing layer is evident beyond $x = 2.75$ in. and the constant velocity lines converged to a point to define the virtual origin. The spreading rate, (db/dx), computed between the velocity ratio (u/u_e) of 0.1 to 0.9, was found to be approximately 0.064 for $M_e = 2.47$ flow, compared to 0.16 for the incompressible flow case.[12] The conventional spreading parameter σ was found to lie between 27 and 29.

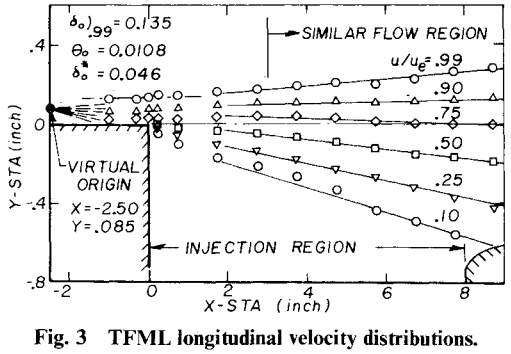

Fig. 3 TFML longitudinal velocity distributions.

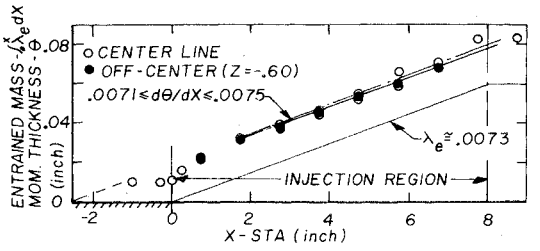

Fig. 4 Comparison of momentum thickness distribution vs entrained mass distribution.

The momentum thickness growth rate closely matched the mass entrainment rate computed from the injection rate as shown in Fig. 4, thereby verifying that the TFML of this investigation was two-dimensional and self-similar. Note that the $d\theta/dx$ of the $M_e = 2.47$ flow is also appreciably smaller; approximately one-fifth the incompressible value.

In order to compare the velocity profiles of the supersonic and the incompressible TFML, the supersonic velocity profile was transformed by the two previously suggested scaling laws. The velocity profile comparison is shown in Fig. 5. It is seen that the integral transformation suggested by Fernandez[7] did not satisfactorily reduce the profile of the present investigation to the incompressible form. The H-D transformation depends on the local density ratio, and the subsonic region is compressed more than the supersonic region. On the other hand, excellent matching of the two profiles was obtained by linear scaling. The present investigation confirmed that the spreading rate is proportional to the density ratio and the momentum thickness growth rate is proportional to the square of the density ratio.[8]

Shear stress distributions (Fig. 6) were computed from the mean flow profiles and found to be very similar to the other mixing layer type of flow[7] when they were plotted against the velocity ratio. The peak value of turbulent shear stress occurred slightly above the dividing streamline near $u/u_e \cong 0.62$. For the truly asymptotic TFML, the locations of maximum shear stress and dividing streamline should coincide. The discrepancy is attributable to the presence of finite initial boundary layer ($\theta/\theta_o \gtrsim 5$). The normalized peak shear stress ($\tau_{max}/\rho_e u_e^2 \lambda_e$) was approximately 0.385 which was slightly higher than the incompressible value of Liepmann and Laufer[12] ($\cong 0.34$) and was constant with streamwise station. Note, however, $\tau_{max}/\rho_e u_e^2$ decreases with increasing Mach number, since λ_e decreases with increasing Mach number.

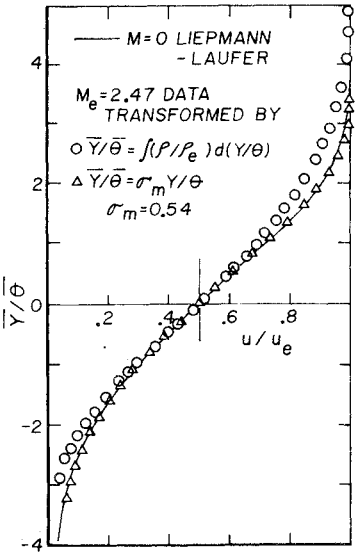

Fig. 5 Linear and integral scaling of supersonic TFML velocity profiles.

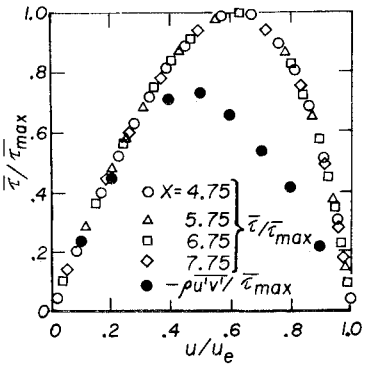

Fig. 6 Shear stress distributions.

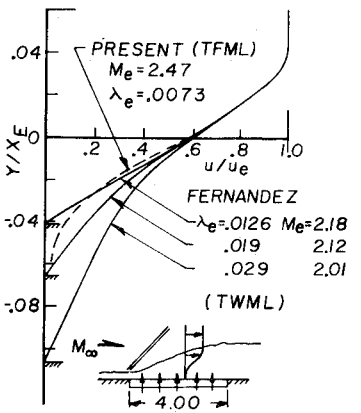

Fig. 7 Comparison of TWML velocity profiles.

The Reynolds stress in the compressible flow consists of two major correlation terms of fluctuating quantities, i.e., $\tau = -\rho\overline{u'v'} - u\overline{\rho'v'}$. The hot-wire measurement of $\overline{u'v'}$ and $\overline{\rho'v'}$ was attempted without success in the present investigation. In order to obtain crude estimates, the total stress was separated into two correlation terms by the assumption $\overline{\rho'v'}/\rho u_L = (\gamma-1)M_L{}^2\overline{u'v'}/u_L{}^2$. The estimated quantities are also shown in Fig. 6. Note, an appreciable $u\overline{\rho'v'}$ contribution is apparent in the supersonic region. Comparison of significant properties between the incompressible and the supersonic mixing layers of the present investigation is listed in Table 1.

Comparison of Supersonic TFML and TWML

Uniform injection of mass into the supersonic turbulent boundary layer (TBL) investigated by Fernandez[7] showed that a flowfield similar to the mixing layer can be created. Fernandez had demonstrated that the velocity profiles of supersonic flow with various blowing rates can be reduced to the subsonic velocity profiles of respective blowing rates by the application of the Howarth-Dorodnitsyn transformation. He terminated the experiments at the blowing rate of 0.029 for which the transformed velocity profile agreed with the incompressible profile of Liepmann and Laufer.[12] It was concluded that the upper limit of the entrainment rate for the supersonic turbulent mixing layer is equal to the incompressible value, $\lambda_e = 0.035$. Then it follows that the momentum thickness growth rate in the similar turbulent mixing layer is independent of Mach number because θ is invariant under the H-D transformation.

The present investigation, conducted in the same wind tunnel used by Fernandez, produced the results contrary to the observation made by Fernandez. The primary difference between two experiments was that the flowfield studied by Fernandez was always bounded by the wall, whereas the present one was free from the wall effects. Therefore, the mixing layer flow created by massive injection into the TBL will be called, in this paper, the turbulent wall mixing layer (TWML) in order to distinguish it from the turbulent free mixing layer (TFML) of the present investigation.

The mass entrainment characteristics of TWML can be examined by observing the velocity profiles of various injection rates in the physical coordinate system. The common reference point is selected at $u/u_e = 0.6$, near the dividing streamline, instead of the wall. Fernandez' data, normalized by the effective distance of the upper layer (X_E), reveal that the velocity profile can be divided into two distinct regions, i.e., above and below the dividing streamline near the sonic point as shown in Fig. 7. The profile in the supersonic region coincides with the TFML form for blowing rate as low as 0.01. The external profiles remain nearly unchanged with further increase in the blowing rate. The forced mass entrainment is confined to the subsonic region between the dividing streamline and the wall. The thickening in the subsonic region is nearly proportional to the injection rate and appears to be an exact inverse of the contraction of the y-coordinate by the H-D transformation. Thus, the TWML is capable of entraining more mass than the fully developed TFML. This is simply an observation of the difference between TWML and TFML. No explanation can be offered at present for the difference in terms of entrainment mechanisms.

Table 1 Comparison between incompressible and supersonic two-dimensional turbulent free mixing layer properties

	Incompressible (Liepmann & Laufer)	Supersonic (M = 2.47) (Present investigations)
dy/dx $(0.10 \leqq u/u_e \leqq 0.90)$	~0.16	~0.064
$d\theta/dx = \lambda_e$	0.035	0.0073
σ	11 ~ 12	27 ~ 29
$\tau_{max}/\lambda_e \rho_e u_e{}^2$	0.34	0.385
$\tau_{max}/\rho_e u_e{}^2$	0.012	0.0028
ρ_w/ρ_e	1.0	0.45
$(\langle u'\rangle/u_e)_{max}$	0.16 ~ 0.18	0.05 ~ 0.06

Turbulent Field Data

The present investigation revealed that at least the following three conditions must be satisfied before the supersonic turbulent mixing layer can be classified as the fully developed asymptotic form; 1) constancy of spreading rate with streamwise distance; 2) turbulent spectra of broadband character with no peak signal; and 3) constancy of total turbulence energy level. The second condition will be discussed later.

The self-similarity of the turbulence field was confirmed by the turbulent spectral surveys made at several stations along the constant velocity ray. The frequency and the spectral intensity (normalized by integrated quantity), were normalized by the mean flow quantity, u_L/θ. Velocity fluctuation spectra, computed by the modal analysis from the data measured along a constant velocity line near the dividing streamline, are shown in Fig. 8.

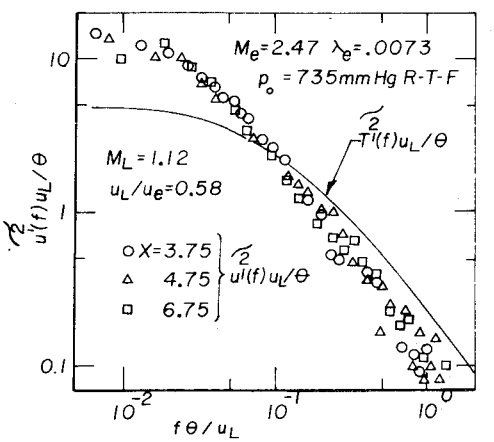

Fig. 8 TFML similar flow spectra.

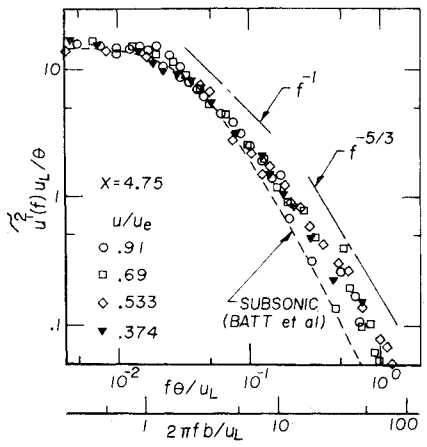

Fig. 9 Comparison of supersonic and incompressible streamwise velocity fluctuation spectra.

The self-similarity is evident. Since the measurements were taken along the constant velocity ray and the momentum thickness was found to grow linearly, that the spectra can be normalized with the local momentum thickness implies that the integral scale of turbulence was also a linear function of streamwise distance ($\Lambda/\theta \cong 3.6$ using Hinze[13]). Spectral distribution was observed to be a broad-band type with no discernible peak. The total turbulent intensity was constant with the streamwise distance after it was corrected for the instrumentation response. The turbulence Reynolds number based on the integral scale ($u'\Lambda/\nu$) varied from about 1000 at the start to 4000 at the end of the investigated shear layer. These facts give credence to the assertion that the flow was fully turbulent and self-similar beyond the longitudinal station $x = 375\,\theta_o$. The representative static temperature fluctuation spectra (solid line) is compared with the velocity fluctuation spectra in Fig. 8. The spectra of temperature fluctuation is much broader than the velocity spectra, implying that more energy is distributed in a higher frequency domain and has a slower decaying structure.

Velocity fluctuation spectra at different locations across the mixing layer reduced to a single curve when they were normalized with the local velocities as shown in Fig. 9. This implied that the characteristic frequency across the mixing layer is inversely proportional to the local mean velocity, u_L. In order to compare the present results with the incompressible turbulent spectra, the frequency and intensity were renormalized with the maximum slope thickness of the mixing layer determined as suggested by Batt et al.[14] The incompressible spectra of Batt et al. agreed in the low frequency range of spectra and the energy carrying component matched near the Strouhal number ($2\pi fb/u_L$) of unity. Within the range of the amplifier response, the final decay of supersonic spectra measured at higher frequencies appears to follow $f^{-5/3}$. However, high-frequency components of incompressible data fall off with -2 power (note this was a low Reynolds number flow), but it was also reported by other investigators[15,16] that the incompressible spectra were also found to decay with $-\frac{5}{3}$ power. Agreement of two spectra when they were normalized by the width of the mixing layer rather than the momentum thickness implies that the u'-field at $M_e = 2.47$ is kinematically similar to that in $M = 0$ flow, especially for the energy carrying eddies.

The static temperature spectra obtained across the shear layer reduced to a single curve when the spectra were normalized with the local mean static temperature $[\tilde{T}'^2(f)(u_e/\theta)(T_e/T_L)$ vs $(f\theta/u_e)(T_L/T_e)]$. The reduced spectra were found nearly identical with the velocity spectra of Fig. 8.

The rms intensities of streamwise velocity and static temperature fluctuation distributions, normalized with the respective local flow properties, are shown in Fig. 10. Scattering of data is inevitable in this type of experiment; therefore, the confidence level of the computed data is somewhat low. However, the ensemble of many data points established a certain trend of the realizable turbulence. The maximum rms intensity of the relative streamwise velocity fluctuation ($\langle u'\rangle/u_L$) was found to be approximately 8–9% of the local mean velocity and occurred near the maximum gradient of the velocity profile. The absolute value of the maximum rms fluctuation was found to be approximately 5–6% of the freestream velocity ($\langle u'\rangle/u_e$) and is shown as the shaded band of the curve. The corresponding peak values in incompressible flow reported by various investigators[12,15,16,20] lie between 16 to 20% of u_e. The general relationship between the remaining velocity fluctuation components (rms of v' and w') in the supersonic TFML is expected to follow the trend observed in the subsonic TFML. Thus it is speculated that the relative kinetic energy of the velocity fluctuation at $M \cong 2.5$ is also expected to be lower than the incompressible value.

The static temperature fluctuation, normalized with the local mean static temperature, peaked in the supersonic side of the layer near the point of maximum gradient of the mean value. The peak rms temperature fluctuation is approximately 8.5% of T_L as shown in Fig. 10b. The plateau near $y/\theta \cong -2$ is speculated to be caused by the difference in the turbulent transport mechanisms between the momentum and the thermal fluctuations. Under the assumption of negligible pressure fluctuation, the temperature fluctuation is precisely a negative of the density fluctuation ($T'/T_L = -\rho'/\rho_L$), but the rms fluctuation of density and temperature are the same.

The streamwise velocity and static temperature fluctuation were found to be highly anticorrelated at the freestream edge of TFML ($R_{\overline{u'T'}} < -0.7$). The correlation approached zero (uncorrelated) near the dividing streamline and become positive in the subsonic region. Relatively high correlation ($R_{\overline{u'T'}} > 0.7$) was observed near $y/\theta \cong -2$.

The combined intensity of all fluctuating modes in supersonic TFML were found large but some amount of energy appeared to have dissipated into thermal energy (mainly from the high-frequency components) as observed in the high temperature fluctuation profile. If T_o' is zero, then $R_{\overline{u'T'}} = -1$. $R_{\overline{u'T'}} > 0$ in the subsonic region implies that T_o' is not only nonzero but also $R_{\overline{u'T_o'}} > 0$ and this could be the result of dissipation. Therefore, it is speculated that the vorticity mode of fluctuation which mainly contributes to the growing of the turbulent field as shown by the kinematic behavior of u'-field is left with relatively low kinetic energy. The observed phenomena may supply a clue to the trend of the spreading rate decreasing with increasing Mach number in the supersonic TFML.

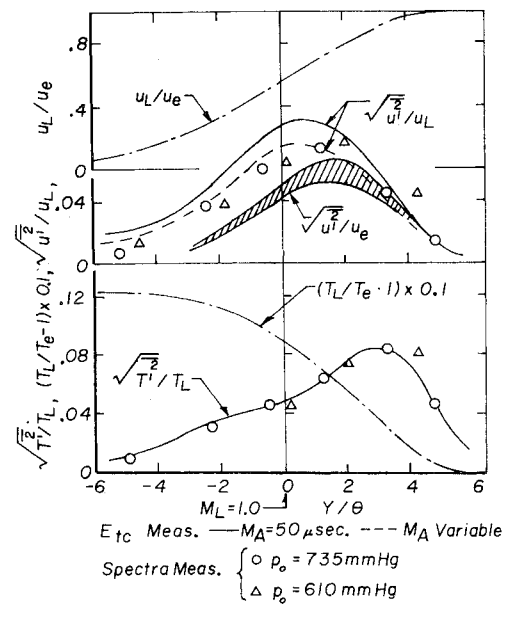

Fig. 10 TFML turbulence intensity distributions.

Recent analysis of turbulent free mixing layer by Oh[17] showed that the proper behavior of supersonic TFML was predicted by introducing the pressure-dilatation correlation $\overline{p'\partial u_j'/\partial x_j}$ in the flow equations. Unfortunately, no valid experimental technique has been developed to measure the pressure fluctuation in the compressible shear flow. Assuming that the pressure fluctuation is constant across the shear layer and the acoustic energy is propagating out without refraction at the shear layer edge,[18] it is possible to measure the pressure fluctuation outside the shear layer. Based on this assumption, the pressure fluctuation is non-negligible, $\langle p'\rangle/\gamma p = 0.015$.[8] However, the order of magnitude comparison of terms in the voltage fluctuation equation showed that the contribution of pressure fluctuation is negligible in the core of the mixing layer for the purpose of data reduction.

The convection velocities of broad-band turbulence across the TFML were compared with the mean velocity and are shown in Fig. 11a. The subsonic data obtained by Wills[11] in the axisymmetric jet mixing layer showed an identical relationship. The subsonic two-dimensional mixing layer results of Wygnanski and Fiedler[19] showed disagreement, however. The convection velocity was consistently lower throughout the TFML.

The qualitative behavior of the presently observed phenomena can be explained by spectral analysis of the convection field. The convection velocities of selected frequency components of turbulence at $u/u_e \cong 0.90$ (region A at maximum unresolved turbulence signal), $u/u_e \cong 0.61$ (region B near the dividing streamline), and $u/u_e \cong 0.25$ (region C in the subsonic region) were measured by using two Hewlett-Packard Wave Analyzers as narrow-bandpass filters before the two signals were correlated and the results are shown in Fig. 11b. At point A, the convection velocity for low frequency components was found to be lower than the mean value and monotonically increasing with frequency. The mean convection velocity at this lateral position was approximately 0.80 u_e and the energy carrying turbulent components were concentrated near the frequency domain of 25 k to 100 kHz. The unresolved power spectral distribution in this frequency domain appeared to decay as f^{-1}. At point B, all frequency components of turbulence were convecting at the same speed. Convection velocities of the turbulence components below the dividing streamline (region C) were decreasing with frequency. Note that the scales of turbulence moving with the mean convection velocity were concentrated near the $f\theta/u_L \cong 0.1$ and the large scale turbulence of the TFML appeared to be moving with relatively constant speed equal to the flow velocity at the

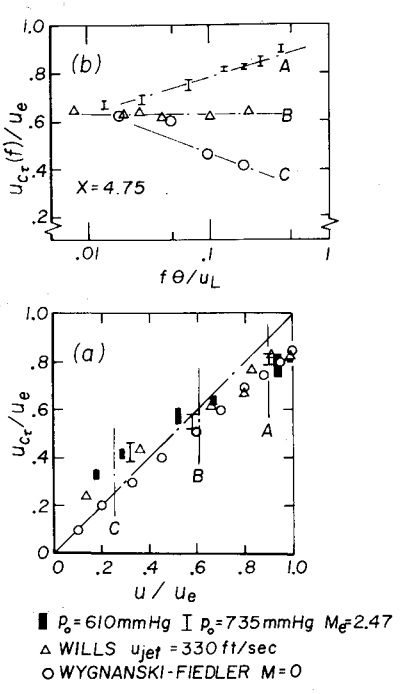

Fig. 11 TFML streamwise turbulent convection velocities.

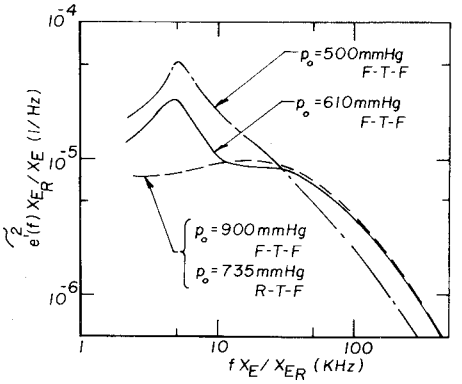

Fig. 12 Comparison of energy spectra with variable total pressures.

dividing streamline across the layer. Jones, et al.[20] also observed qualitatively the same trend in the incompressible two stream mixing layer.

Results of Wills[11] and the present investigations indicate that the switching point of the relative velocity occurs very close to the dividing streamline of the TFML, suggesting that the large-scale turbulence is created in the vicinity of the dividing streamline where the production rate, $\tau(\partial u/\partial y)$, is maximum. The variation of the convective velocity with frequency also indicates that the small-scale turbulence, which is more susceptible to the local environment, is produced by interaction of mean velocity gradient and large scale turbulence[13] as convected downstream.

Development of Turbulence Structure of TFML

When hot-wire surveys were conducted at $p_o = 610$ mmHg, a peaking of signal near 5 kHz appeared in the turbulence spectra. The cause of this peculiarity was traced to the upstream conditions, flow instability or some Reynolds number dependent disturbance in the boundary layer, influencing the downstream flow.

In order to observe the sequential development of turbulence structure, the dependence of turbulent spectra on the total pressure (Reynolds number) variation was investigated in the TFML. The unresolved turbulent energy spectra were normalized with the total turbulence energy and shown in Fig. 12. The boundary layer was tripped with a strip of fine grain sandpaper for the tests conducted with $p_o = 500$, 610, and 900 mmHg. As pressure increases, there is a marked decrease in the 5 kHz peak together with a progressive development of high-frequency components. The presence of large periodic wave of decreasing intensity with increasing total pressure was also detected by auto-correlation measurement, which confirmed the shift which occurred in the turbulent spectra.

The signal peaking was also eliminated when the operation of the tunnel was restored to the total pressure of one atm ($p_o = 735$ mmHg) and the boundary-layer trip was replaced with a strip of coarse grain sandpaper. The entire spectra were found to be identical with the data taken with $p_o = 900$ mmHg. Self-similarity of the turbulence field was evident in these measurements.

The disappearance of spectral peaks with increasing Reynolds number and with boundary-layer trip roughness implies that the structure of fully developed supersonic TFML consists of a randomly fluctuating field with no concentration of high intensity large-scale wave motion in a preferred frequency range. On the other hand, Brown and Roshko[21] observed the existence of quasi-periodic large-scale motion in the incompressible TFML, which indicates a marked difference between subsonic and supersonic turbulent mixing layers.

Conclusions

The present investigation revealed that the turbulent free mixing layer strongly depends upon the compressibility of the

supersonic flow. The supersonic TFML was found to possess characteristics similar to those of the incompressible TFML but their magnitudes were considerably lower.

It was found that the wall bounded mixing layer, created by the massive injection into the turbulent boundary layer, could entrain more mass than the free mixing layer created by the natural process. The thickening of the TWML below the dividing streamline was proportional to the injection rate.

References

[1] Maydew, R. C. and Reed, J. F., "Turbulent Mixing of Axisymmetric Compressible Jet (in the Half-Jet Region) with Quiescent Air," SC-4764 (RR), March 1963, Sandia Corp., Albuquerque, N. Mex.

[2] Roshko, A. and Thomke, G. L., "Results of Pilot Experiment on Supersonic Free Shear Layers," Rept. DAL, A10-290-AAEO-8337, Oct. 8, 1968, McDonnell Douglas Astronautics Co., St. Louis, Mo.

[3] Sirieix, P. M. and Solignac, J. L., "Contribution a L'Etude Experimental de la Couch de Melange Turbulent Isobare d'un Ecoulement Supersonique," T. P. 327, 1966, Office Nationale d'Etudes et de Recherches Aerospatiales, Genèse, Belgium.

[4] Korst, H. H. and Tripp, W., "The Pressure on a Blunt Trailing Edge Separating Two Supersonic Two-Dimensional Air Streams of Different Mach Number and Stagnation Pressure but Identical Stagnation Temperature," *Proceedings of the Fifth Midwestern Conference on Fluid Mechanics,* University of Michigan, Ann Arbor, Mich., April 1957, pp. 187–199.

[5] Crane, L. M., "The Laminar and Turbulent Mixing of Jets on Compressible Fluids—Part I," *Journal of Fluid Mechanics,* Vol. 3, Oct. 1975, pp. 81–92.

[6] Alber, I. E., "Integral Theory for Turbulent Base Flows at Subsonic and Supersonic Speed," Ph.D. thesis, 1967, Dept. of Aeronautics, California Institute of Technology, Pasadena, Calif.

[7] Fernandez, F. L., "Two-Dimensional Viscous Flows with Large Distributed Surface Injection, Parts I, II, and III," Ph.D. thesis, 1969, Dept. of Aeronautics, California Institute of Technology, Pasadena, Calif.

[8] Ikawa, H., "Turbulent Mixing Layer Experiment in Supersonic Flow," Ph.D. thesis, 1973, Dept. of Aeronautics, California Institute of Technology, Pasadena, Calif.

[9] Gran, R. L., "Step Induced Separation of a Turbulent Boundary Layer," Ph.D. thesis, 1970, Dept. of Aeronautics, California Institute of Technology, Pasadena, Calif.

[10] Kistler, A. L., "Fluctuation Measurements in a Supersonic Turbulent Boundary Layer," *Physics of Fluids,* Vol. 2, May–June 1959, pp. 290–296.

[11] Wills, J. A. B., "On Convection Velocities in Turbulent Shear Flow," *Journal of Fluid Mechanics,* Vol. 20, Pt. 3, Nov. 1964, pp. 417–432.

[12] Liepmann, H. W. and Laufer, J., "Investigations of Free Turbulent Mixing," TN 1257, 1947, NACA.

[13] Hinze, J. O., "Turbulence—An Introduction to its Mechanism and Theory," McGraw Hill, New York, 1959, pp. 61, 268.

[14] Batt, R. G., Kubota, T., and Laufer, J., "Experimental Investigation of the Effect of Shear Flow Turbulence on a Chemical Reaction," AIAA Paper 70-721, San Diego, Calif., 1970.

[15] Spencer, B. W. and Jones, B. G., "Statistical Investigation of Pressure and Velocity Fields in the Turbulent Two Stream Mixing Layer," AIAA Paper 71-613, Palo Alto, Calif., 1971.

[16] Yule, A. J., "Two-Dimensional Self Preserving Turbulent Mixing Layers at Different Freestream Velocity Ratios," R & M No. 3863, March 1971, Aeronautical Research Council, London.

[17] Oh, Y. H., "Analysis of Two-Dimensional Free Turbulent Mixing," AIAA Paper 74-594, Palo Alto, Calif., 1974.

[18] Kovasznay, L. S. G., "Turbulence in Supersonic Flow," *Journal of the Aeronautical Sciences,* Vol. 20, Oct. 1953, pp. 657–674.

[19] Wygnanski, I. and Fiedler, H. E., "The Two-Dimensional Mixing Region," *Journal of Fluid Mechanics,* Vol. 41, Pt. 2, April 1970, pp. 327–361.

[20] Jones, B. G., Planchon, H. P., and Hammersley, R. J., "Turbulent Correlation Measurements in a Two Stream Mixing Layer," *AIAA Journal,* Vol. 11, Aug. 1973, pp. 1146–1150.

[21] Brown, G. L. and Roshko, A., "On Density Effects and Large Structure in Turbulent Mixing Layers," *Journal of Fluid Mechanics,* Vol. 64, Pt. 4, 1974, pp. 775–816.